

This article appeared in a journal published by Elsevier. The attached copy is furnished to the author for internal non-commercial research and education use, including for instruction at the authors institution and sharing with colleagues.

Other uses, including reproduction and distribution, or selling or licensing copies, or posting to personal, institutional or third party websites are prohibited.

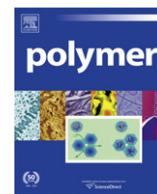
In most cases authors are permitted to post their version of the article (e.g. in Word or Tex form) to their personal website or institutional repository. Authors requiring further information regarding Elsevier's archiving and manuscript policies are encouraged to visit:

<http://www.elsevier.com/copyright>



Contents lists available at ScienceDirect

Polymer

journal homepage: www.elsevier.com/locate/polymer

Forced assembly and mixing of melts via planar polymer micro-mixing

Doyoung Moon, Kalman B. Migler*

Polymers Division, National Institute Standards and Technology, Gaithersburg, MD 20899, United States

ARTICLE INFO

Article history:

Received 14 December 2009

Received in revised form

26 April 2010

Accepted 29 April 2010

Available online 7 May 2010

Keywords:

Forced assembly

Mixer

Microfluidic

ABSTRACT

The ability to force immiscible polymers into specific, targeted structures would enable the generation of blends with tailored performance by exploiting the intimate relationship between structure and blend properties. Here we present a strategy for the forced assembly of immiscible polymers into targeted structures via development of a planar polymer micro-mixer (PPMM). The PPMM drives streams of molten polymer through mixing chambers, which are fabricated from metal shims that contain flow channels. By stacking the shims, complex 3D mixing flows can be generated. The advantages of this mixing technology include sample sizes significantly less than traditional micro-mixers (<100 mg), simple reconfiguration of the flow geometry, and optical access to the flow. Most significantly, it offers a path towards targeted blend structures rather than the more typical domain/matrix or random co-continuous ones. We observe the creation of multi-layers and coaxial cylinders in the first five mixing units, beyond that that interfacial tension and non-ideal flow tends to force the creation of mixed domain/matrix structures. The PPMM, along with the recently developed multi-sample micro-slit rheometer, is expected to be a key component of the “polymer processing lab-on-a-chip”.

Published by Elsevier Ltd.

1. Introduction

¹The blending of immiscible polymers by melt mixing is widely used in the polymer industry as a means to create materials with superior properties [1]. Significant research is devoted to the development of new polymers, their blending strategies, the resulting structure and the ultimate properties. It is well known that specific structures can enhance application specific properties; for example, a multi-layer structure may be desired to reduce gas transport [2], a co-continuous structure may be desired for a polymer scaffold pre-cursor for tissue engineering [3] and a domain/matrix structure is utilized to improve properties such as brittleness [4]. There are two issues associated with the development of new immiscible blends materials that we address in the current work. The first is the difficulty in generating complex and targeted structures. The second is the frequent gap between the quantity of materials available during the development of new polymers and the quantity needed for typical laboratory scale mixers. In the present work, we present a new strategy – based on a planar polymer micro-mixer (PPMM) – to create targeted structures from immiscible polymers. A significant benefit of this method in the materials development stage

is that the PPMM is that the sample mass is orders of magnitude less than traditional polymer mixing technology and significantly smaller than even traditional micro-mixing.

2. Background

Conventional mixing technologies include both active and passive mixers. Active mixers include twin-screw extruders and mixing bowls [5,6]. Recent advances in active micro-scale mixers include the recirculating mixer by Son [7]. An example of a passive mixing technology is a single screw extruder followed by passive mixing elements which split and recombine (SAR) the flow stream numerous times. There are a few forced assembly methods already in existence in which engineered flow fields efficiently mix the polymers to create specific blend structures. Chaotic advection has been utilized to create a multi-layer structure. In one implementation, Zumbrun et al. utilized two stir rods of circular cross-section and the rotation modes of the stir rods are altered in a fashion known to induce chaotic flow [8–10]. They observed a progression of morphologies, from a multi-layered structure to derivative ones such as multi-layer with holes, co-continuous and droplet/matrix. In a second class of forced assembly, a multi-layer structure was achieved by a SAR concept – flow from two separate extruders each containing a mutually immiscible polymer is combined and then flowed through a series of n SAR mixing elements – the total number of layers is 2^n . Through proper design and balance of the viscosities,

* Corresponding author. Tel.: +1 301 975 4876; fax: +1 301 975 4924.

E-mail address: kalman.migler@nist.gov (K.B. Migler).

¹ Official contribution of the National Institute of Standards and Technology; not subject to copyright in the United States.

a uniform multi-layer structure can be achieved [11]. These multi-layer structures can be engineered to possess spectacular optical and gas barrier properties [2] and also serve as model systems to study interfacial phenomena such as adhesion, interdiffusion, surface-nucleated crystallization and slippage [12–15]. The above methods produce multi-layers as their sole targeted structure and require 10 g–1000 g of material.

Microfluidic mixing technologies fall at the other extreme from the high viscosity, temperature and mass throughput regime of polymer blend processing as they were initially developed to scale-down characterization and separation methods for limited quantity biological samples. A large literature has developed to address the question of mixing in microfluidic devices because the typical low viscosity fluids, which are simple to mix in macro-scale flows by large Reynolds number turbulence, are in the low Reynolds number regime in microfluidic geometries and one must resort to low Reynolds mixing strategies [16–18]. To date, microfluidic methods have not been applied to polymer blends.

A desirable feature of microfluidic methods is the relative ease in which complex flow geometries can be produced to manipulate

flow for specific purposes — extensional flow regions, mixing regions, droplet formation regions and chemical reaction regions have all been demonstrated. Typical construction of microfluidic mixers is based on lithographic techniques adapted from the semiconductor industry [16–18] and there are two general classes of microfluidic mixers: passive and active.

In active mixers external fields such as pressure, temperature, electrohydrodynamic, dielectrophoretic, electrokinetic, magneto-hydrodynamic or acoustic drive the flow. Among active mixers, pulsed injection to produce alternating flow is a simple way to generate good mixing in a microchannel by controlling the flow rates or the pressures at the inlets of the channels without any moving parts. The mixing is obtained by the fluid deformation of the consecutive parabolic flow. This mixing effect was conceived for electrokinetic flow [19] and experimentally investigated by Glasgow and Aubry [20,21] by using aqueous solutions; the degree of mixing was analyzed by a computational fluid dynamics which included diffusive effects. A similar flow pattern in binary immiscible polymers can be obtained by a special arrangement of a material charge in the barrel of a flow tester or a capillary

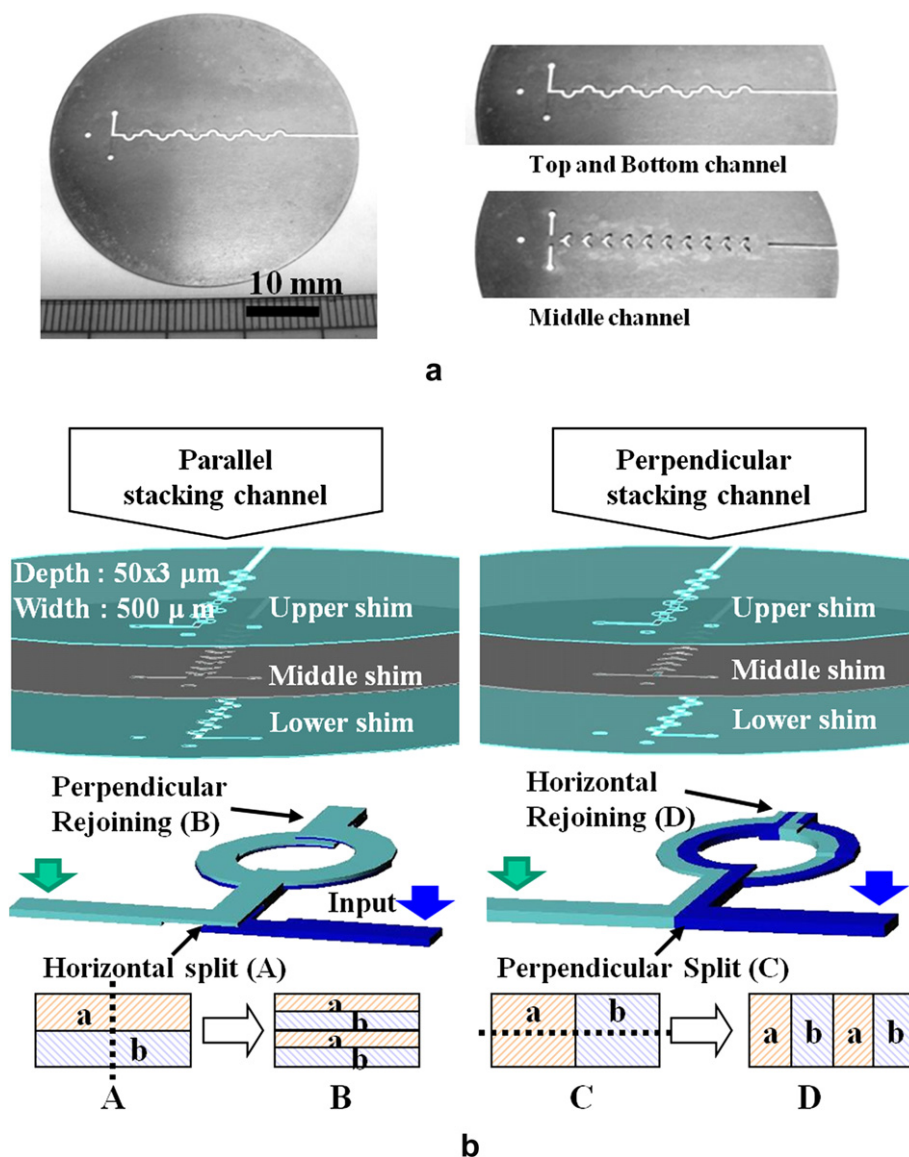


Fig. 1. Split and Recombine (SAR) mixer. (a) Photographs of the metal shims containing flow channels. (b) Schematic of three stacked shims and the resulting idealized flow in a configuration to generate parallel (left) and perpendicular (right) multi-layers.

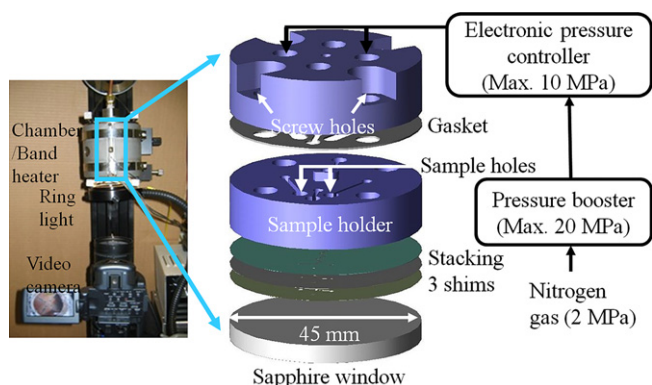


Fig. 2. Schematic of the planar polymer micro-mixer (PPMM) in the split and recombine mode and a photograph of the experimental set-up.

rhometer. The method involves stacking compression molded disks of two different materials in alternating order in the barrel [22]. The extrudate cross-section revealed an ordered coaxial structure.

Passive mixers have the advantage of simpler fabrication [17] and make use of geometric features in the flow geometry. Various mixing mechanisms have been adapted for passive micro-mixers such as flow focusing, flow separation, chaotic advection and splitting/recombination flow (SAR mixer). The SAR mixer is reliable and effective under low Reynolds number ($Re < 1$) conditions, as is typical in polymer melts processing. The SAR mixer can produce micrometer multi-layer structures simply by adding mixing units as the number of layers increases exponentially [23]. In addition, the SAR mixer can achieve mixing by chaotic advection [24–26] for microchannels in a low Reynolds number regime [27,28].

Here, we utilize concepts from both microfluidic and polymeric mixing to develop the PPMM. We demonstrate the PPMM in both a passive mode with three stacked shims and in an active mode with either one or three shims in conjunction with a staircase pressure profile. We target several structures: multi-layers, domain/matrix and multiple coaxial cylinders. For the multi-layer structures, we demonstrate methods to produce sheets that are both parallel and perpendicular to the sample geometry as well as methods to create both a constant multi-layer thickness and a gradient layer thickness. Similar to the recently developed multi-sample micro-slit rheometer (MMR) [29], it is based on the simple pressure driven flow of molten polymer through metal shims which contain channels for directing the polymer flow. It is flexible in that the flow geometry can be reconfigured by removing the shims and replacing with others that contain different flow patterns. We ultimately envision the development of a “polymer processing lab-on-a-chip” technology, where complex manipulation, mixing and measurement all take place in one environment with volume requirements orders of magnitude lower than typical methods.

3. Mixer design

3.1. General platform

²The PPMM is designed to for high temperature operation, mechanical simplicity, cleanability and optical access. The various

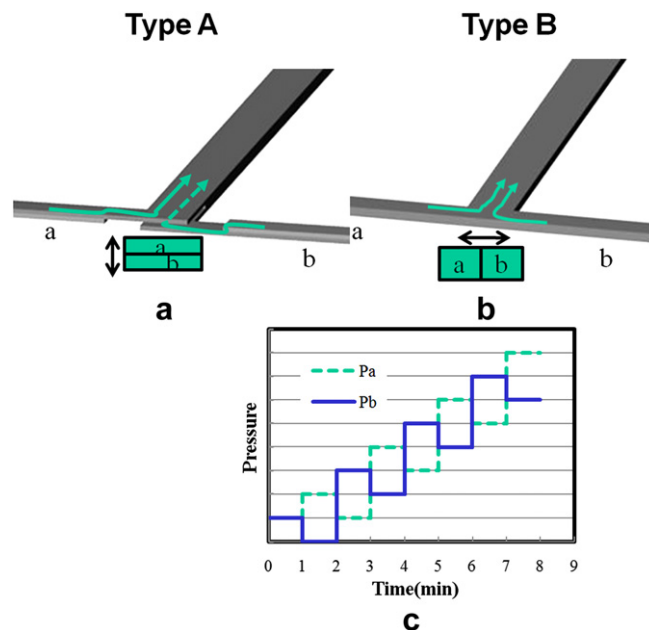


Fig. 3. Two types of T-channels in an example of active mixing. (a) Parallel and (b) perpendicular joining at a T-junction. (c) Sketch of staircase pressure profiles where P_a and P_b are the inlet pressures with a constant difference between them of (700 kPa).

low viscosity microfluidic mixing implementations presented in the previous section are not simply amenable to polymer melts due to their inability to function at the required temperatures and pressures. Our design is an extension of the recently developed MMR in which gas pressure forces multiple molten polymers to flow through straight channels that have been laser cut into a thin ($\approx 50 \mu\text{m}$) metal shim which is sandwiched between a sapphire window and a sample holding chamber. The PPMM differs first in that the shims are designed so that the different polymers can mix with each other as they traverse the channels. In the simplest case, the shims bring two polymer streams together in a T-junction. In the more general case, we utilize multiple stacked shims to achieve flexibility in the flow – using the analogy of a building where

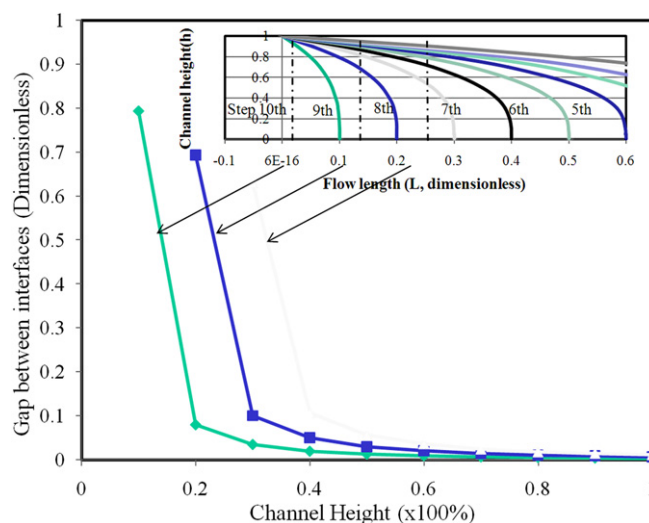


Fig. 4. layer thickness change along channel length (0.1, 0.2, 0.3 position, length scale is 0–1) in alternating feeding condition. Inset shows interface shapes of ten alternating feeding in a slit channel (bottom line is a center of the channel, power law fluid, $n = 0.5$).

² Certain equipment, instruments or materials are identified in this paper in order to adequately specify the experimental details. Such identification does not imply recommendation by the National Institute of Standards and Technology nor does it imply the materials are necessarily the best available for the purpose.

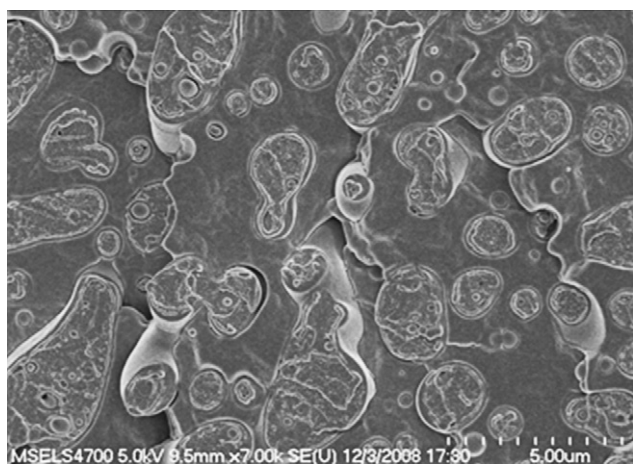


Fig. 5. Morphology of PS/PP blend compounded by a mini-extruder at 20.94 rad/s (100 rpm) and 200 °C for 10 min.

a shim represents a story in the building and a channel in a shim represents a corridor, we can say the polymer can flow through corridors in a floor, it can flow through shafts from one story to another, and it can flow through multi-story atriums. The second major modification that we make for the MMR is to allow independent pressure control of each sample holder, which is utilized in our demonstration of active mixing.

3.2. Passive SAR mixer

Three-dimensional flow channels are required to form a SAR mixer because the flow must be split, reoriented and recombined. The two-component SAR mixer is formed by stacking three stainless steel shims (50 μm in thickness each) in which channels are laser cut (FCT Assembly, 2 μm cutting resolution) as shown in Fig. 1. The shims are sandwiched between a sample holder and a sapphire window (See Fig. 2) and sealed by the mechanical forces of six screws supported at a retaining ring (not shown in Fig. 2). Nitrogen gas drives the molten polymer from the two sample holes into the flow channels. The flow pattern can be viewed from the window side and recorded by video camera.

Fig. 1 shows the three-dimensional flow geometry that we utilize for the SAR mixer. There are two configurations; one which is designed to create multi-layers parallel to the shims and the other perpendicular. Regardless, the gas pressure to polymer A and polymer B at the sample holder is identical at any point in time (see Fig. 1). The parallel multi-layer is created by a series of n SAR units; in each unit the flow is split into two channels with a perpendicular cut, the height of each resultant channel is decreased in half, and then flow is recombined into one channel by placing one flow stream on top of the other. A similar scheme is employed for the perpendicular multi-layer structure but the axes of the splitting and recombination are rotated 90°. The parallel multi-layer configuration has a lower target thickness for a given number of SAR units because the initial thickness is less. Careful examination of Fig. 1 reveals that

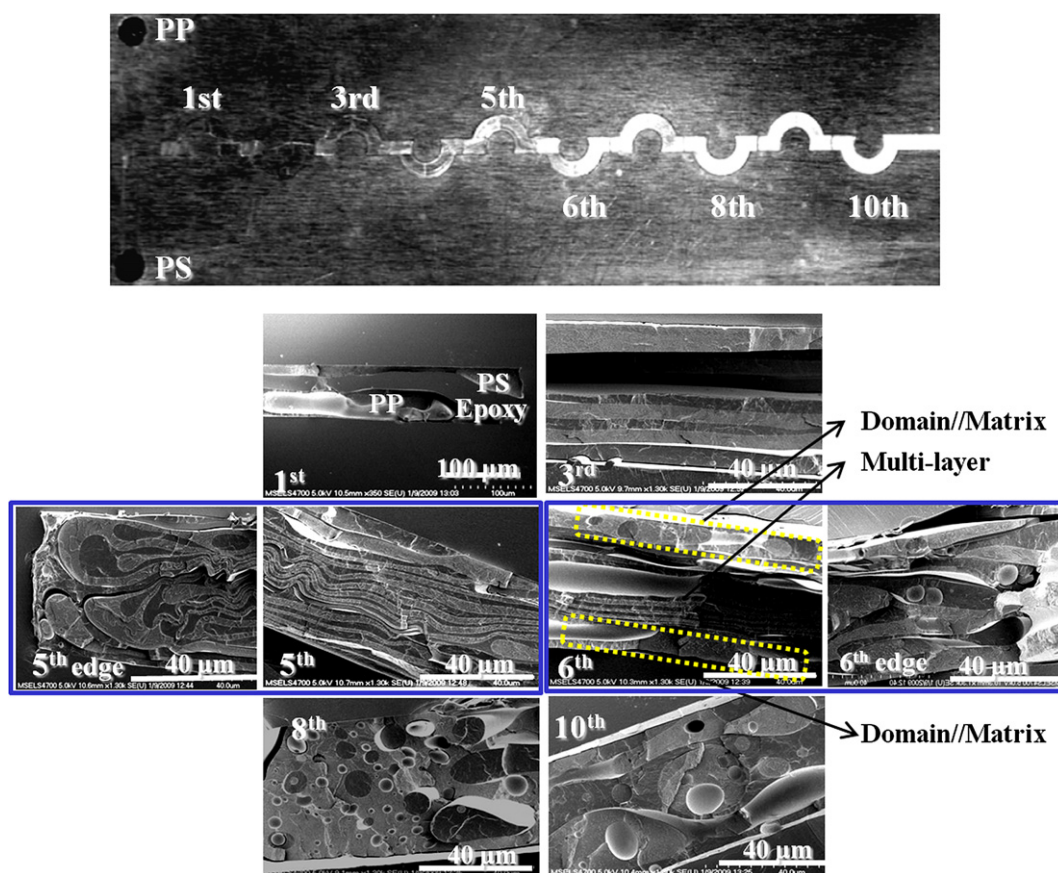


Fig. 6. Split and recombine mixer in parallel multi-layer configuration. (a) Video micrograph of the flow channel – only the flow through the shim in contact with the sapphire window is visible. (b) SEM images of the cross-sections of the PS/PP samples at the 1st, 3rd, 5th, 6th, 8th and 10th mixing units. Whiteness of the flow at the 5th downstream mixing unit in (a) reveals a breaking-up of structure from multi-layer to domain/matrix morphology, as confirmed in (b).

only three distinct shim patterns were used to create the two mixing configurations because the top and bottom shims are all identical - just their orientation varies.

3.3. Active mixer

In an active mixer, we structure the blend by dynamically controlling the inlet pressures at A and B. As we demonstrate, this provides a strategy to create structures that have a continuous gradient in layer thickness. We demonstrate this active mixer by supplying staircase pressure profiles to the inputs of A and B that are 180° out of phase with respect to each other (See Fig. 3) so that the pressure difference between the two inputs alternates in sign. There are two configurations for the shims, both based on a T-junction, one is called parallel (Fig. 3a) because the initial joining of polymers A and B occurs parallel to the shims and the other is called perpendicular (Fig. 3b). For the perpendicular configuration, the width to depth ratio of the channel is five. For the parallel configuration, the channel is formed by stacking three shims; the top and bottom are 50 μm thick and the middle is 25 μm. One can expect the mixing patterns and resultant morphologies of the blend to differ based on the joining direction of the flows at the T-junction.

To demonstrate how this flow profile can generate a gradient in layer thickness, we consider a simplified situation of a simple slit and quasi-steady state flow. The velocity profile of a power law fluid [30] is:

$$u(y) = \frac{2n+1}{n+1} V \left[1 - \left(\frac{2|y|}{H} \right)^{\frac{n+1}{n}} \right] \quad (1)$$

where $u(y)$ is the velocity at channel height y from a channel center, V is the average flow velocity, H is the channel height and n is the power law index. Equation (1) can be written in simple form by introducing the appropriate dimensionless parameters $U(h)$ and h instead of $u(y)$ and y :

$$U(h) = 1 - h^{\frac{n+1}{n}} \quad (2)$$

Assuming the initial flow profile is flat at the fluid inlet and ignoring the effect of the interfacial tension, the position of the fluid interfaces at each alternating time step would be obtained by determining the distance each fluid interface has traversed along the channel length.

$$L_i(h) = U(h)t_i \quad (3)$$

Where $L_i(h)$ and t_i are respectively the interface position at channel height h and time t at alternating feeding step i . The inset of Fig. 4 shows the interface pattern obtained by Eq. (3) for ten alternating steps and power law index, $n = 0.5$. The widths of the layers in the channel can be calculated from Eq. (3) by obtaining finding the distance between adjacent interfaces $\Delta h_j (= h_{i+1} - h_i)$ between time step t_{i+1} and t_i at a given channel length. Fig. 4 shows the layer-widths between interfaces at channel lengths 0.1, 0.2 and 0.3 (channel length scale is 0–1). The layer-width is a maximum at the center and decreases continuously as a function of distance to the wall. Though the channels in this study are rectangular, the analysis here should capture the major structural trends.

3.4. Sample holder and pressure handling unit

The PPMM must produce the temperatures and pressures necessary to melt polymers and force them through the channels. Fig. 2 shows the sample holding unit which consists of two stainless steel plates; an upper one that interfaces with the high pressure

tubes and a lower one that contains the four 50 μL sample holders. (In this study, only two of the four holders were used.) The lower sample plate has four channels on its top surface to guide the gas from the holes of the upper sample plate (which are connected by a high pressure tube to a high pressure nitrogen source) to the four sample holders of the lower plate. The four sample holders are connected, through the top plate plumbing, to individual pressure sources. The upper and lower plates are sealed by three stacked gaskets (polyimide film/copper shim/polyimide film). Fig. 2 shows our system for high pressure gas generation – it consists of a typical nitrogen gas cylinder/regulator (maximum 2 MPa) which feeds into a pressure booster (Curtiss-Wright Corporation, Sprague S-486-JN-30) and then into an electronic high pressure controller/regulator (Tescom, ER3020SI-1/26-1025D24A-568). The sample holders sit directly on top of the inlet holes in the shim slits. The assembly containing the sample holders, multi-shim channels and sapphire window are placed inside a stainless steel chamber which is wrapped in a band heater; the temperature is limited by the polyimide sheets to approximately 400 °C. Consequently, the high pressure and temperature capability of the platform make it suitable for most thermoplastics.

4. Experimental procedure

The polymer pair utilized in these experiments is polystyrene (PS) (Styron 666D, Dow Chemical) and polypropylene (PP) (Exceed 4062, Exxon) chosen in because their viscosities closely match each other over the shear rate range (0.1–200) s^{−1} in shear rate at 200 °C [8] and there is image contrast between the two. For the passive mixing (SAR) experiments, a linearly increasing pressure profile (138 kPa/min) up to a maximum 6.9 MPa (at 50 min) at 200 °C was used in order to roughly maintain a constant averaged flow rate

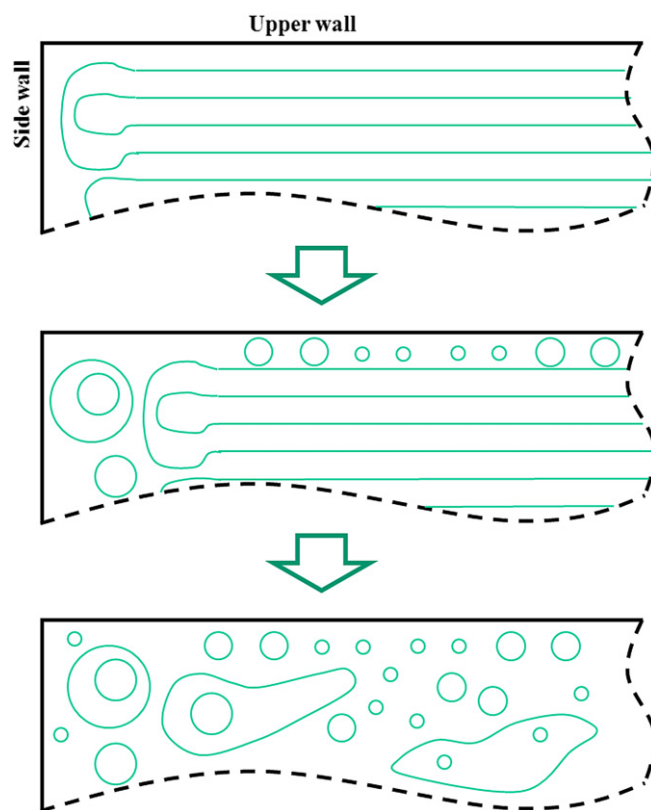


Fig. 7. Schematic diagram of morphology evolution in a rectangular channel with SAR mixing configuration for an immiscible binary blend.

through the successive mixing elements. For the active mixing experiment, the period of the staircase is 1 min with step jump amplitude of 700 kPa.

Air bubbles were eliminated by first melting the samples in the sample holder inside a vacuum oven at 190 °C for 30 min. We note that short duration heating (just long enough to melt the polymers) followed by mechanical packing produced qualitatively similar results to those presented in this manuscript. During the loading and the assembly of the sample holder/shims/sapphire window assembly, the alignment of the three shims and sample holder are important. We simply place a few drop of distilled water between three shims and sample holder as a temporary adhesive which allowed manual alignment – the water was removed quickly by vaporization in the 200 °C sample chamber before applying any driving pressure. A video camera was used for the direct examination of the mixing pattern and scanning electron microscopy (Hitachi, S-4700, SEM) was used to view the strips. Molded strips are detached manually from the shims, embedded in epoxy and cryo-fractured prior to SEM observation. The shims are cleaned with toluene for later reuse.

For purposes of comparison, we also melt-mixed the PS/PP in a conventional twin-screw mini-mixer at 20.94 rad/s (100 rpm) and 200 °C for 10 min. We allowed a small quantity to extrude, quenched it and measured its blend structure by SEM as shown in Fig. 5. We observe a generic domain/matrix structure with average sizes $(1.7 \pm 1.6) \mu\text{m}$. The domain sizes of Fig. 5 are measured and counted manually and processed by Excel function (Microsoft), STDEV.

5. Results and discussion

We first discuss the parallel stacking configuration, (shim design on bottom-left of Fig. 1). A top-down video micrograph taken at the end of the experiment is shown in Fig. 6a and SEM micrographs from six mixing units are shown in Fig. 6b. Up until the 5th mixing unit, a multi-layer pattern is observed although the layer thicknesses are not uniform. At the 5th unit the morphology varies from multi-layer in the central region of the cross-section to curved structures at the left and right regions. At the 6th mixing unit, the multi-layer pattern remains in the central region, but discrete domains are now visible on the sides. At the 8th and 10th unit, the

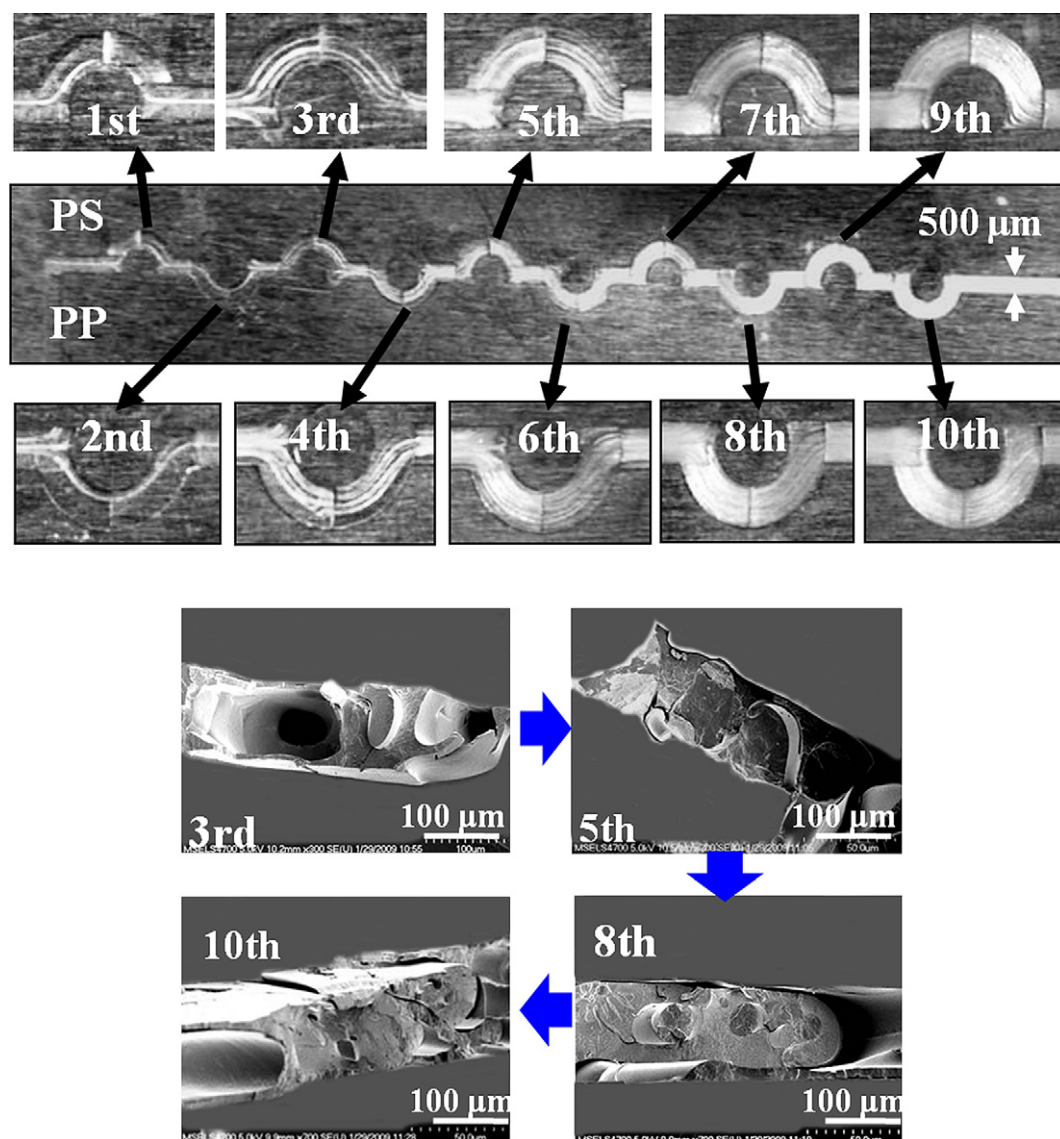


Fig. 8. Split and recombine mixer in perpendicular multi-layer configuration. (a) Video micrograph of the flow channel – only the flow through the shim in contact with the sapphire window is visible. (b) SEM images of the cross-sections of the PS/PP samples at the 3rd, 5th, and 8th mixing units. The embedding epoxy is cropped out of the images for purposes of clarity.

morphology is changed completely to the domain/matrix or co-continuous pattern. This morphology change can be confirmed by the whitening of the flow as seen in the video micrograph in Fig. 6a. The white lines visible near the sides of the 4th and 5th mixing units are caused by regions where there are highly curved structures that scatter light. The mixture becomes increasingly white at progressively larger n indicating the transitions from multi-layer to curved. We note that the whitening seen in Fig. 6a is visible during the flow process and the degree of whitening does not change considerably during the cool-down phase. Thus the preponderance of the highly curved structures seen in the SEM is most likely caused during the processing as opposed to the cool-down phase (where some annealing will nevertheless occur).

The morphology evolution of the blend in the parallel stacking configuration has been summarized in Fig. 7. In a rectangular channel, the edge of the multi-layer cannot maintain its rectangular shape due to interfacial tension and secondary flows in the corner. Therefore, the multi-layer structure breaks up first in the corner as shown in 5th edge SEM image of Fig. 6b. In the corner of a rectangular channel, edges of layers fuse and are folded into each other, consequently, a large domain can be separated easily from the inner multi-layer because a separated domain is thermodynamically more preferential than the multi-layer structure. This morphology transition propagates continuously and irreversibly in the inner direction of the channel. We also note in Fig. 6b that the multi-layer breaks up in the 5th and 6th mixing unit in the immediate vicinity of the top and bottom walls before breakup occurs in the central region. While the shear rate is greatest in the near wall regions, the flow velocity is least, thus the allowing more time for any potential disturbance in the flow to distort the layers and initiate a breakup [10,31]. We hypothesize that the disturbance that initiates the breakup is the sudden area change in cross-section that occurs in each mixing unit.

Note that the distribution of the domain sizes of the mixture in the 8th and 10th sections is bimodal (many small domains and a few large domains). This is consistent with a previous observation that when the multi-layer structure is broken during flow, a population of smaller particles is formed because of the Rayleigh instability and a second population of larger particles is formed by

a relaxation mechanism [14] of multi-layer breakup and the corner effect as previously described.

The perpendicular stacking configuration is the second passive mixer that we examined with our immiscible blend of PP/PS (shim layout shown in bottom-right of Fig. 1). In the video micrograph of the flow pattern, Fig. 8a, we observe an increasing number of white lines as a function of mixing unit until approximately the 5th, when they can no longer be resolved. The presence of a white line in the flow, as early as the first unit, indicates that the interface between the PP and PS is curved rather than flat. Therefore, one can conclude that the number of layers, and the degree of mixing, is increasing through the first five units, but not as simply as the idealized picture of Fig. 1. Fig. 8b shows the cross-sectional SEM results at the 3rd, 5th, 8th and 10th mixing units. The idealized multi-layers are not present even at the 3rd unit, but rather a cylindrical morphology is observed. The interfacial tension and non-ideal SAR flow between the PS and PP hinder the formation of the rectangular multi-layers.

In both passive configurations, the intermediate structures are reflective of the ideal configurations while the ultimate structures are domain/matrix structures. These observations can be attributed to two primary factors. First, the idealized structures of Fig. 1 would occur only under ideal SAR flow conditions. The effects of non-idealized flow become magnified as a result of the repetitive nature of the mixing units. Second, the structure is ultimately unstable with respect to the formation of domains, the capillary number $Ca \approx 1$, based on the typical operating condition of the experiments (viscosity ≈ 6000 kPa at $\dot{\gamma} \approx 1$ s⁻¹ [12], interfacial tension between PP and PS of approximately 0.06 N/m [32], average flow velocity of 10 μ m/s and slit height of 50 μ m) which means that domains can in principle grow to a size of roughly 50 μ m.

The active mixer based on the staircase pressure profiles into the PS and PP sample chambers (Fig. 9a and b) provides a means for generating a different class of structure. One advantage of the active mode over passive is that one can create blends with structural variation in the flow direction by applying temporally varying pressure fields, such as those applied here. In the perpendicular configuration (Fig. 9a:I), the variation of structure along the flow direction can be seen in the photograph. In the idealized structure,

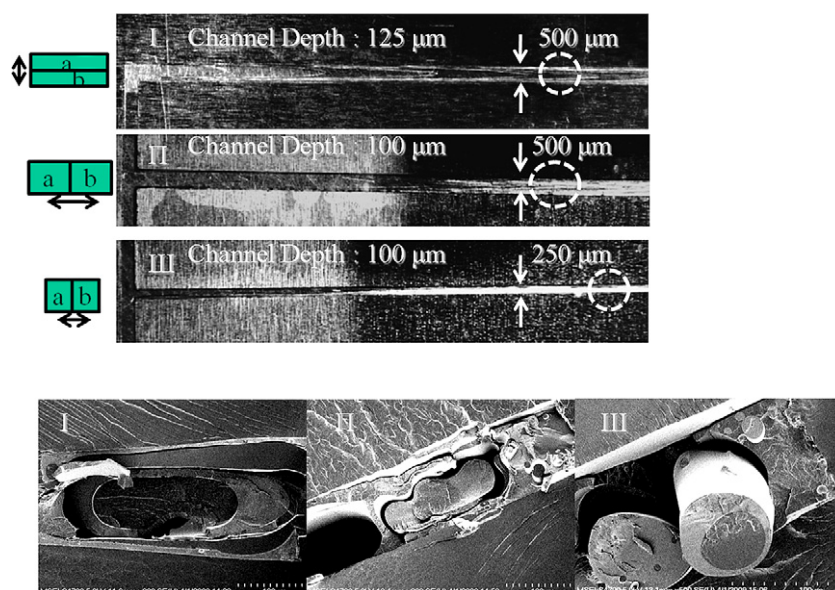


Fig. 9. T-junction active mixer. (a) Flow patterns and (b) SEM photographs of the cross-sections of the PS/PP blend samples for the pressure profile shown in Fig. 3. Dotted circles in (a) show the positions where cross-sections are imaged in (b). I: T-channel with a parallel joining junction, 500 μ m in width, 125 μ m (three shims) in depth, II: simple T-channel, (perpendicular joining) 500 μ m in width, 100 μ m in depth, III: simple T-channel, 250 μ m in width, 100 μ m in depth.

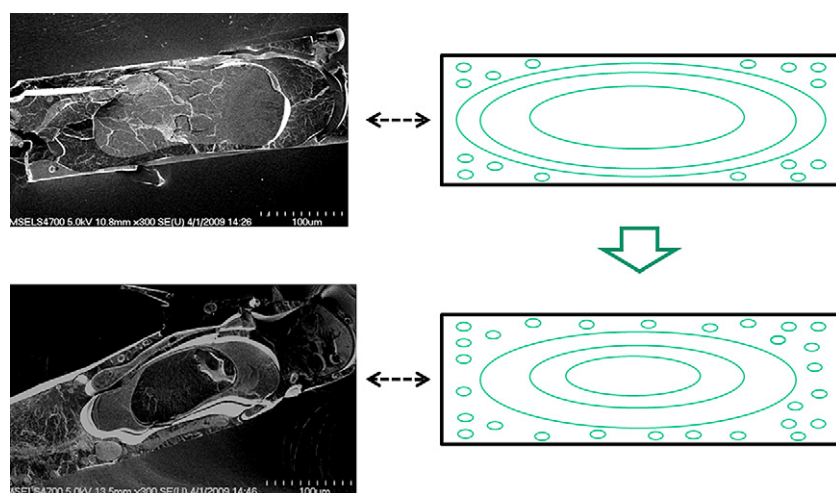


Fig. 10. Morphology evolution in a rectangular channel of an alternating feeding mixer for an immiscible binary blend (Parallel configuration, left is SEM micrographs, right is schematic diagrams of the morphology).

each parabolic curve is the front of PP penetrating into PS, or vice-versa. In the SEM micrograph (Fig. 9b:I), one can observe a single coaxial structure. In the case of the lateral configuration, the parabolic front is observed to migrate from one side of the channel to the other as the injection pressure changes from one polymer to the other. This migration leads to multiple coaxial structures, as observed in the SEMs of Fig. 9b(II and III). The video micrograph shows that further downstream, the flow front is white, indicating a breakup of the coaxial structures of Fig. 9a(II and III).

Fig. 10 shows more detail about the morphology progress of the parallel configuration. As explained with Fig. 4, the scissoring action of the interfaces make the layer thickness near the wall thin enough to break up the layer structure effectively. The portion of thin layers across the whole cross-section increases gradually along the channel length, therefore, the region of the fine domain/matrix also increases gradually along the channel. Further, as shown in Fig. 4, only few numbers of coaxial interfaces can be found because most layers are squeezed near the wall. Regarding such a mixing characteristics, we can say that this alternating mixer produces a gradient in the layer thickness and thus an uneven mixing profile across the cross-section of the channel. A Newtonian fluid is predicted to have less of a gradient in this mixer because the velocity profile is not plug-like.

6. Summary and conclusions

We have demonstrated that small quantities (<100 mg) of immiscible polymers can be intimately mixed in a planar polymer micro-mixer (PPMM) and that one can utilize the flow to force specific structural morphologies in the blend. The advantages of this technology over existing mixing technologies include smaller material quantity (approximately 50 mg compared to 5 g), and, ability to structure the blend into targeted structures and the easy reconfiguration of the flow field through modification of the shim channels. We demonstrated this concept in a model passive mixer in a 3D split and recombine flow, as well as in an active mixer with the T-channel geometry. The results indicate that good mixing was achieved. Furthermore, the creation of specific and targeted morphologies such as multi-layers with constant thickness, multi-layers with gradients in layer thickness, long cylinders or coaxial cylinder, and of course the domain/matrix or co-continuous morphology during the mixing process is achievable. The SEM micrographs at the consecutive mixing units allow one to reconstruct the evolution of the morphology. In the SAR mixer, the multi-

layer structures break up first in the side corner of the rectangular channel, next, near the wall, then propagate rapidly to the inner section. In the alternating feeding mixer, breakup of multi-layer occurs intensively at the vicinity of the channel wall, then the region of the fine domain/matrix propagates gradually along the channel downstream.

Further development of the PPMM requires advancements across several areas: flow modeling, mechanical testing and determination of confinement effects. For flow modeling, realization of the full potential for targeted structures will require flow modeling incorporating interfacial tension and elastic effects. Due to the relative ease of designing and cutting flow channels, one can imagine an iterative process between modeling, fabrication and testing.

The second required development of micro-mechanical testing is facilitated by the fact that the PPMM can mold samples into specific forms – such as dogbone – that are amenable to downstream testing of mechanical properties. This would be important in order to close the loop between structure, processing and mechanical properties. While mechanical testing of the blend structures is beyond the scope of this manuscript, it is an essential element to the overall technological platform. It is hoped this work, along with micro-molding in general, will motivate the development of micro-scale mechanical testing instruments.

The third area for future development is to utilize wall and confinement effects. We note that compared to traditional macro-scale mixing, much of the sample is in close proximity to a wall. Indeed, it has been shown in the case of simple shear flow between parallel plates, that the morphology of a blend can be strongly influenced by confinement effects when the size of a typical domain is similar to that of a typical flow channel. New structures were observed such as strings, “pearl-necklaces” and layered droplets [33–35]. In the present case, the flow is driven by pressure and so there is a range of shear rates across the gap. It would be quite interesting to determine whether new structures can be generated in pressure driven flow.

We envision that the PPMM will be a component of a “polymer processing lab-on-a-chip” technology, where complex measurement and processing operations take place over length and mass scales that are orders of magnitude smaller than previous methods. Beyond structuring of blends, we anticipate that with the platform developed can be adapted to an assorted of measurement challenges in polymer processing including polymeric droplet dynamics, interfacial tension, compatibilization and interfacial reactions.

References

- [1] Paul DR, Newman S. Polymer blends. New York: Academic Press; 1978.
- [2] Wang H, Keum JK, Hiltner A, Baer E, Freeman B, Rozanski A, et al. Confined crystallization of polyethylene oxide in nanolayer assemblies. *Science* 2009;323:757–60.
- [3] Washburn NR, Simon CG, Tona A, Elgandy HM, Karim A, Amis EJ. Co-extrusion of biocompatible polymers for scaffolds with co-continuous morphology. *Journal of Biomedical Materials Research* 2002;60:20–9.
- [4] Kyu T, Saldanha JM, Kiesel MJ. Toughness enhancement in polycarbonate/polymethylmethacrylate blend via phase separation. In: Utracky LA, editor. Two phase polymer systems. NewYork: Hanser Publ. Munich; 1991. p. 259–75.
- [5] Hold P. Theory and practice of polymer mixing. In: Utracky LA, editor. Two phase polymer systems. NewYork: Hanser Publ. Munich; 1991. p. 43–67.
- [6] Cheremisinoff NP. Polymer mixing and extrusion technology. New York: Marcel Dekker, Inc; 1987.
- [7] Son Y. Development of a novel microcompounder for polymer blends and nanocomposite. *Journal of Applied Polymer Science* 2009;112:609–19.
- [8] Zumbrunnen DA, Inamdar S. Novel sub-micron highly multi-layered polymer films formed by continuous flow chaotic mixing. *Chemical Engineering Science* 2001;56:3893–7.
- [9] Zumbrunnen DA, Inamdar S, Kwon O, Verma P. Chaotic advection as a means to develop nanoscale structures in viscous melts. *Nano Letters* 2002;2:1143–8.
- [10] Zumbrunnen DA, Subrahmanian R, Kulshreshtha B, Mahesha C. Smart blending technology enabled by chaotic advection. *Advances in Polymer Technology* 2006;25:152–69.
- [11] Mueller C, Kerns J, Ebeling T, Nazarenko S, Hiltner A, Baer E. Microlayer coextrusion: processing and application. In: Coates PD, editor. Polymer process engineering 97. Ashgate Publishing; 1997. p. 137–57.
- [12] Zhao R, Macosko CW. Slip at polymer-polymer interfaces: rheological measurements on coextruded multilayers. *Journal of Rheology* 2002;46:145–67.
- [13] Zhao R, Macosko CW. Polymer-polymer mutual diffusion via rheology of coextruded multilayers. *Aiche Journal* 2007;53:978–85.
- [14] Jin Y, Hiltner A, Baer E. Fractionated crystallization of polypropylene droplets produced by nanolayer breakup. *Journal of Polymer Science Part B-Polymer Physics* 2007;45:1138–51.
- [15] Jin Y, Rogunova M, Hiltner A, Baer E, Nowacki R, Galeski A, et al. Structure of polypropylene crystallized in confined nanolayers. *Journal of Polymer Science Part B-Polymer Physics* 2004;42:3380–96.
- [16] Hardt S, Drese KS, Hessel V, Schonfeld F. Passive micromixers for applications in the microreactor and mu TAS fields. *Microfluidics and Nanofluidics* 2005;1:108–18.
- [17] Nguyen NT, Wu ZG. Micromixers – a review. *Journal of Micromechanics and Microengineering* 2005;15:R1–16.
- [18] Zhang CS, Xing D, Li YY. Micropumps, microvalves, and micromixers within PCR microfluidic chips: advances and trends. *Biotechnology Advances* 2007;25:483–514.
- [19] MacInnes JM. Computation of reacting electrokinetic flow in microchannel geometries. *Chemical Engineering Science* 2002;57:4539–58.
- [20] Glasgow I, Aubry N. Enhancement of microfluidic mixing using time pulsing. *Lab on A Chip* 2003;3:114–20.
- [21] Glasgow I, Lieber S, Aubry N. Parameters influencing pulsed flow mixing in microchannels. *Analytical Chemistry* 2004;76:4825–32.
- [22] Cohen A, Schroeder JR. Morphological analysis of the viscosity anomaly for Pp Ps blends. *Journal of Rheology* 1990;34:685–704.
- [23] Schonfeld F, Hessel V, Hofmann C. An optimised split-and-recombine micromixer with uniform 'chaotic' mixing. *Lab on A Chip* 2004;4:65–9.
- [24] Liu RH, Stremmer MA, Sharp KV, Olsen MG, Santiago JG, Adrian RJ, et al. Passive mixing in a three-dimensional serpentine microchannel. *Journal of Micro-electromechanical Systems* 2000;9:190–7.
- [25] Niu XZ, Lee YK. Efficient spatial-temporal chaotic mixing in microchannels. *Journal of Micromechanics and Microengineering* 2003;13:454–62.
- [26] Ottino JM. Mixing, chaotic advection, and turbulence. *Annual Review of Fluid Mechanics* 1990;22:207–53.
- [27] Coleman JT, Sinton D. A sequential injection microfluidic mixing strategy. *Microfluidics and Nanofluidics* 2005;1:319–27.
- [28] Xia HM, Wan SYM, Shu C, Chew YT. Chaotic micromixers using two-layer crossing channels to exhibit fast mixing at low Reynolds numbers. *Lab on A Chip* 2005;5:748–55.
- [29] Moon D, Bur AJ, Migler KB. Multi-sample micro-slit rheometry. *Journal of Rheology* 2008;52:1131–42.
- [30] Agassant J-F, Avenas P, Sergent J-PH, Carreau PJ. Polymer processing: Principles and modeling. Carl Hanser Verlag; 1991.
- [31] Joshi AS, Zumbrunnen DA. Computational clarifications of experimental blend morphology transitions in immiscible polymer melts organized by chaotic advection. *Chemical Engineering Communications* 2006;193:765–81.
- [32] Macaebas PHP, Demarquette NR. Morphologies and interfacial tensions of immiscible polypropylene/polystyrene blends modified with triblock copolymers. *Polymer* 2001;42:2543–54.
- [33] Migler KB. String formation in sheared polymer blends: coalescence, breakup, and finite size effects. *Physical Review Letters* 2001;86:1023–6.
- [34] Pathak JA, Davis MC, Hudson SD, Migler KB. Layered droplet microstructures in sheared emulsions: finite-size effects. *Journal of Colloid and Interface Science* 2002;255:391–402.
- [35] Van Puyvelde P, Vananroyea A, Cardinaelsa R, Moldenaers P. Review on morphology development of immiscible blends in confined shear flow. *Polymer* 2008;25:5363–72.